PHYSICAL REVIEW B

CONDENSED MATTER

THIRD SERIES, VOLUME 50, NUMBER 19 15 NOVEMBER 1994-I

# Transport in polyaniline networks near the percolation threshold

Reghu M., C. O. Yoon, C. Y. Yang, D. Moses, Paul Smith, and A. J. Heeger
*Institute for Polymers and Organic Solids, University of California at Santa Barbara, Santa Barbara, California 93106*

Y. Cao
*UNIAX Corporation, 5375 Overpass Road, Santa Barbara, California 93111*
(Received 20 June 1994)

The self-assembled network of conducting polyaniline (PANI), protonated by camphor sulfonic acid (CSA), in a matrix of insulating polymethylmethacrylate (PMMA) has a remarkably low percolation threshold. The critical volume fraction ($f$) of the PANI-CSA phase segregated in PMMA is inferred from the concentration dependence of the conductivity, $f_c \approx 0.003$ (0.3%). The conductivity at room temperature near the percolation threshold is quite high, $3 \times 10^{-3}$ S/cm. Transmission-electron microscopy (TEM) results are in agreement with the percolation threshold inferred from the transport data; the TEM micrographs show that the connectivity of the PANI-CSA network decreases rapidly for $f < 0.005$. Near room temperature, the positive temperature coefficient of resistivity ($\rho$), a feature typical of the intrinsic metallic nature of PANI-CSA, is retained in the networks. At lower temperatures, $\rho(T)$ exhibits a temperature-dependence characteristic of variable range-hopping transport, $\rho(T) \propto \exp[(T_0/T)^{\gamma}]$, with the exponent increasing from $\gamma = 0.25$ to 1 upon decreasing the volume fraction of PANI-CSA from $f = 1$ to $f_c$. This systematic increase in $\gamma$ results from transport on the fractal structure and to the related superlocalization of the electronic wave functions. Below the percolation threshold, the temperature dependence of the resistivity is like that of granular metals with $\gamma \approx 0.5$, consistent with the morphology and microstructure seen in the TEM micrographs. The positive magnetoresistance shows a maximum upon decreasing the volume fraction of PANI-CSA in agreement with effective-medium theory. Analysis of the magnetoresistance indicates that the localization length near the percolation threshold is approximately 25 Å at 4.2 K.

## I. INTRODUCTION

The transport properties of classical percolating systems have been studied in detail for many years.[1] In such systems, the critical volume fraction ($f_c$) for percolation is approximately 16% for globular conducting objects dispersed in an insulating medium in three dimensions. Experimental and theoretical studies of polymer composites filled with metal[2,3] or carbon fiber,[4] have shown that the percolation threshold decreases when the aspect ration ($A$) of the conducting object increases, where $A$ is the ratio of the length ($L$) to diameter ($\delta$).[5]

The study of transport properties of conducting polymer blends, consisting of fibril-shaped conducting objects, is in a relatively early stage of investigation.[6-13] The formation of self-assembled networks in conducting polymer blends provides an alternative class of percolating systems. Because the multiply connected, phase-separated morphology is the lowest-energy configuration, the critical volume fraction of conducting material required to reach the percolation threshold can be quite low.[10,11] Transport on such fractal networks is of fundamental interest, but poorly understood. Moreover, since the homogeneity and processibility of conducting polymer blends is superior to that of fiber-loaded polymer composites, these all-polymer materials are of technological interest.

We have reported initial results on the transport properties of conducting polyblends of polyaniline–camphor sulfonic acid (PANI-CSA) in polymethyl-methacrylate (PMMA).[10,11] The PANI-CSA networks in PANI-CSA/PMMA blends exhibit an extremely low percolation threshold and a continuous increase of conductivity, $\sigma(f)$, while retaining the mechanical properties of the matrix polymer.[10,11] Homogenous films of any size and shape can be easily fabricated either by codissolving the conducting PANI-CSA and a suitable matrix polymer in a common solvent and casting onto a substrate or by melt processing the blend.[10] The intrinsic metallic nature of PANI-CSA (as inferred from the positive temperature coefficient of resistivity) is retained upon dilution to low volume fractions ($f \approx 0.003$), a feature which is not ob-

 

served in other conducting polymer blends. Moreover, the positive and linear temperature dependence of thermopower remains unchanged upon dilution to 0.6% volume fraction of PANI-CSA.[11(c)] Thus, the transport data imply the formation of a self-assembled interpenetrating fibrillar network of high quality PANI-CSA during the course of liquid-liquid phase separation.[10] The implied networks were directly imaged through transmission-electron microscopy (TEM) studies of the PANI-CSA blends.[10(b)]

The technological prospects of conducting polymer blends for use in a variety of applications has stimulated a more detailed study of these materials with a goal of achieving a deeper understanding of the role of material processing on the morphology and thus on the transport properties. In the present work, we have extended the temperature dependence of the resistivity and magnetoresistance to a wider range of volume fractions of PANI-CSA (from $f=0.0005$ to 1) on samples prepared under quasiequilibrium conditions such that the percolation threshold is $f_c \approx 0.003$, reduced from the previous value by nearly an order of magnitude. We have carried out an extensive study of the temperature dependence of the electrical conductivity and resistivity, and magnetoresistance in such PANI-CSA/PMMA blends over the wide range of volume factions, focusing especially on concentrations near the percolation threshold.

Interpretation of the systematic change in $\gamma$ as a function of the volume fraction of PANI-CSA suggested superlocalization of the electronic wave functions on the fractal network for concentrations near the percolation threshold.[11] In the present study, we have succeeded in reducing the percolation threshold to $0.3\pm0.05$ vol% PANI-CSA. Again, we find that the value of $\gamma$ systematically increases from 0.25 (at $f \approx 0.8$) to $\gamma \approx 1$ upon decreasing the volume fraction of PANI-CSA to the percolation threshold. Because of the relatively high conductivity of the phase separated PANI-CSA in PMMA, we are able to extend the measurements to blends with concentrations well below $f_c$. Below the percolation threshold, we find $\gamma \approx 0.5$, typical of that observed in granular metals and consistent with the morphology seen in the TEM micrographs.

## II. EXPERIMENT

Polyaniline–camphor sulfonic acid solutions are prepared by dissolving the emeraldine base form of PANI and CSA at 0.5 molar ratio of CSA to phenyl-N repeat unit in *m* cresol.[10] This solution is then mixed in appropriate ratio with a solution of PMMA in *m* cresol. Films of thickness 20–60 $\mu$m were obtained by casting the blend solution onto a glass plate. After drying at 50 °C in air for 24 h, the polyblend film was peeled off the glass substrate to form a free-standing film for transport measurements.

The principal difference between the samples used in the present and earlier studies is that the molecular weight of the PMMA is lower in the present case. This enables greater mobility of the macromolecules during the process of liquid-liquid phase separation (carried out slowly at 50 °C), thereby enhancing the diffusion of PANI-CSA in PMMA. As a result, the blends more closely approach the morphology associated with the minimum-energy morphology of the PANI-CSA self-assembled network. In this way, the percolation threshold has been reduced to 0.3%, nearly an order of magnitude lower than observed in the earlier measurements.

Four-terminal dc resistivity and magnetoresistance measurements were carried out from 300 K down to 1.4 K in a cryostat containing a superconducting magnet (0–10 T) using a computer-controlled measuring system.[14] Electrical contacts were made with conducting carbon paint. To avoid sample heating at low temperatures, the current source was adjusted at each temperature so that the power dissipated into the sample was less than 1 $\mu$W. Moreover, for measurements below 4.2 K, the samples were immersed directly in liquid helium to ensure excellent thermal contact. The linearity was checked by measuring voltage vs current, and the resistivity was obtained from the slope of the straight line. Temperature was measured with a calibrated platinum resistor (300–40 K) or a calibrated carbon-glass resistor (40–1.2 K) and controlled by the computer.

## III. RESULTS AND DISCUSSION

The previous work in PANI-CSA/PMMA blends demonstrated clearly that the electrical transport properties of this novel percolating medium are rather different from those observed in more traditional systems.[11] Recent theoretical models of superlocalization,[15,16] multifractal localization,[17,18] multiple percolation,[13] and high-field magnetotransport[19] near the percolation threshold have provided additional stimulus to carefully study the transport properties of the PANI-CSA network, especially at low volume fractions near the percolation threshold. Moreover, the TEM micrographs of the samples indicate connected networks at volume fractions well below 1%; i.e., at significantly lower PANI-CSA content than previously reported. This is consistent with the use of lower molecular weight PMMA and slower evaporation of the solvent at a modest temperature with the goal of controlling the liquid-liquid phase separation so as to allow the system to more nearly approach equilibrium. The resulting improvements in material quality have enabled the temperature dependence of conductivity measurements and magnetoresistance measurements in samples containing volume fractions of PANI-CSA as low as 0.02%.

### A. Electron microscopy and conductivity near percolation threshold

Transmission-electron microscopy micrographs of blends made from 0.5% and 0.25% PANI-CSA in PMMA are shown in Figs. 1(a) and 1(b) [see Ref. (10b) for details on the preparation of samples for imaging by TEM]. The details of the PANI-CSA network can be seen quite clearly. Figures 1(a) and 1(b) resemble the typical scenario imagined for a percolating medium[1] with "links" (PANI-CSA fibrils), "nodes" (crossing points of the links), and "blobs" (dense, multiply connected re-

gions). The distance between the nodes and the typical diameter of the blobs is assumed to be of the order of the percolation correlation length ($\xi_p$).[1] The TEM photograph of the sample containing 0.5% PANI-CSA indicates that $\xi_p \sim 400-800$ Å. In the sample containing 0.5% PANI-CSA numerous links, with diameters of about 100–500 Å, are clearly visible; while for the 0.25% sample there are rather few links between the nodes and blobs. This indicates that the network is unstable and tends to break up at volume fractions below 0.5% PANI-CSA in PMMA.

The phase separation of PANI-CSA in PMMA into an interconnected network morphology is important for obtaining relatively high conductivity and a low percolation

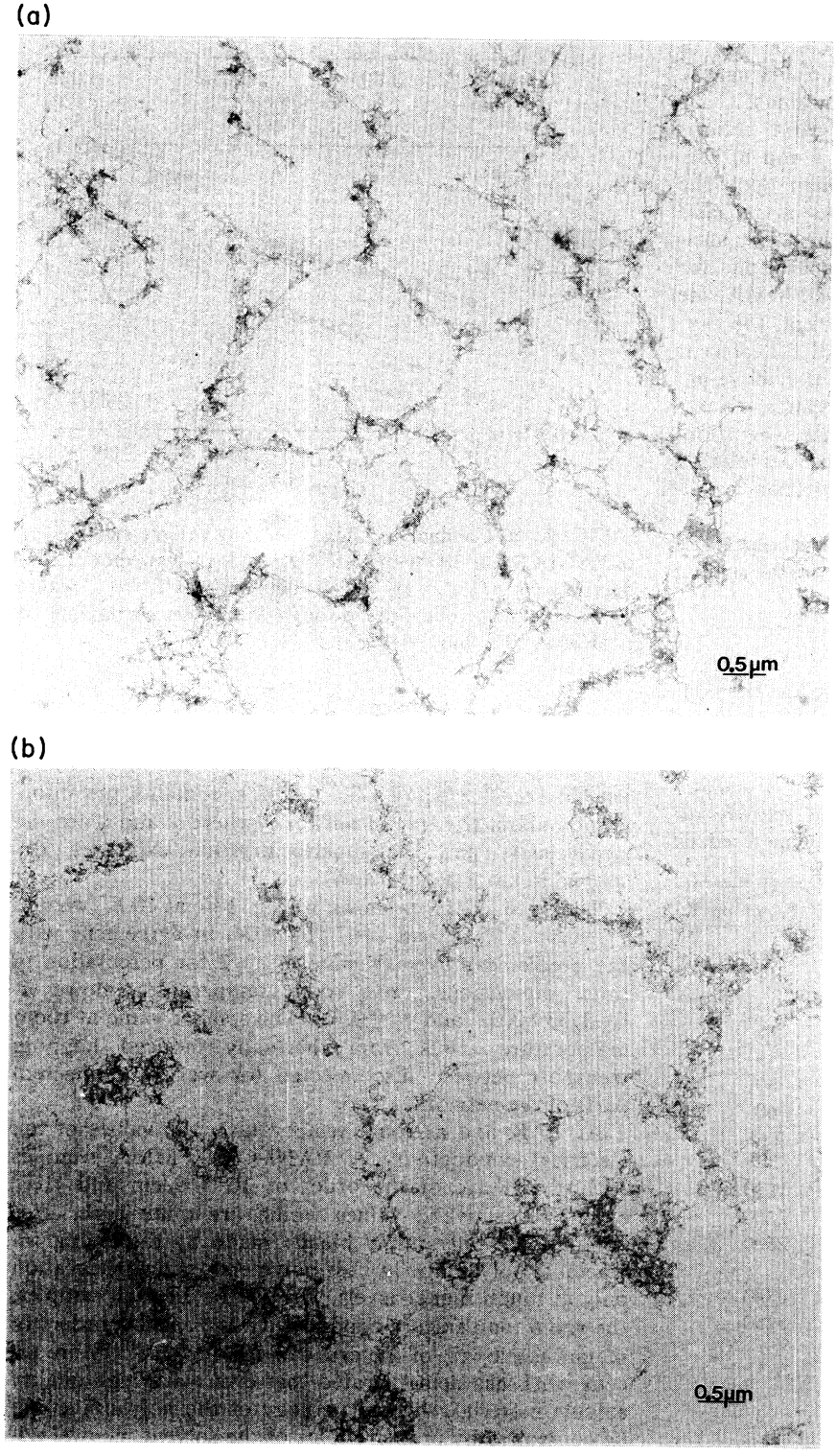


FIG. 1. Transmission-electron micrographs of extracted PANI-CSA/PMMA polyblend films containing (a) $f=0.005$ and (b) $f=0.0025$ PANI-CSA.

threshold. The network morphology is superior to a homogeneous solution of conducting chains in the host material; for in the case of such a solid solution, the electrical conductivity of the chains would be seriously limited by the Peierls instability and by one-dimensional localization.

The micrographs, Figs. 1(a) and 1(b), suggest the existence of a minimum diameter of order a few hundred Ångstrom units for the connecting links. Although the origin of this minimum dimension is not understood in detail, it appears that when the surface to volume ratio of the PANI-CSA segregated regions becomes too large, the connected network structure cannot be maintained.

The relationship between conductivity and volume fraction of PANI-CSA is shown in Table I and in Fig. 2(a). This relationship is critically dependent upon the nature of mass distribution among the links, nodes, and blobs in the sample which in turn is determined by various parameters involved in the sample preparation: for example, the molecular weight of PANI and PMMA, the viscosity of the polyblend solution, the solvent, the drying temperature, etc. The samples used in the present work were prepared by optimizing some of the above parameters with the intent of allowing the system to approach equilibrium during liquid-liquid phase separation. The morphology of the network near the percolation threshold is sensitive to the sample preparation conditions.

In order to identify the percolation threshold more precisely, we have attempted to fit the data to the scaling law of percolation theory,[1]

$$\sigma(f)\approx\sigma_T|f-f_c|^t\,, \tag{1}$$

where $\sigma_T\approx(r_h)^{\zeta_R}\sum(r_h)$, which is interpreted as the conductance for each basis unit; "$t$" is the critical exponent ($t\approx1$ in two dimensions and $t\approx2$ in three-dimensions);

TABLE I. Room temperature conductivity and resistivity ratio of PANI-CSA/PMMA blends at various volume fractions ($f$) of PANI-CSA.

| $f$ | $\sigma$(300 K) S/cm | $\rho$(4.2 K)/$\rho$(300 K) |
|---|---|---|
| 1 | 200–400 | 1.3–10 |
| 0.8 | 140 | 11 |
| 0.67 | 110 | 13 |
| 0.5 | 66 | 18 |
| 0.33 | 21 | 19 |
| 0.12 | 9 | 30 |
| 0.08 | 4 | 60 |
| 0.04 | 1.8 | 210 |
| 0.02 | 0.7 | 710 |
| 0.015 | 0.4 | 1830 |
| 0.012 | 0.22 | 2200 |
| 0.010 | 0.17 | 2600 |
| 0.008 | 0.12 | |
| 0.006 | 0.074 | 3780 |
| 0.004 | 0.014 | 5250 |
| 0.003 | 0.003 | |
| 0.002 | 0.0012 | |
| 0.001 | $10^{-4}$ | |
| 0.0005 | $10^{-5}$ | |

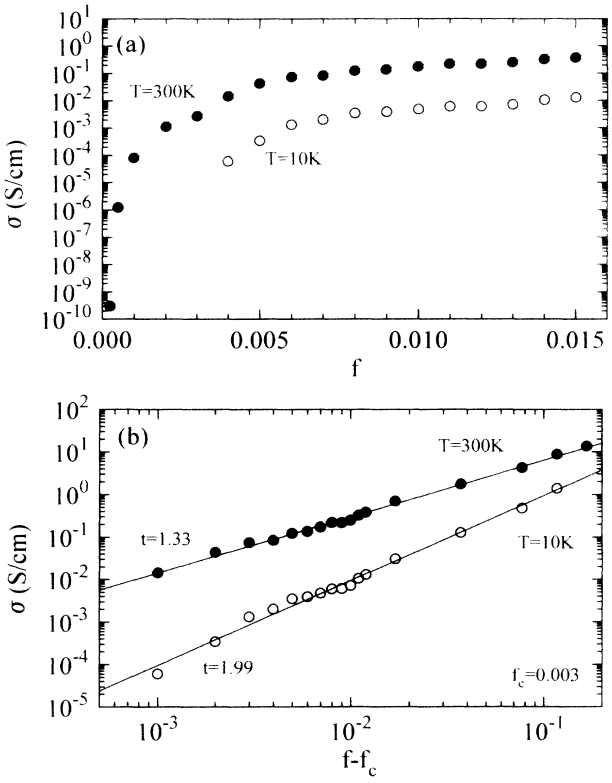


FIG. 2. (a) Conductivity ($\log_{10}$ scale) vs volume fraction ($f$) of PANI-CSA at 300 K and at 10 K; (b) $\log_{10}$-$\log_{10}$ plot of conductivity vs $(f-f_c)$ at 300 K (●) and 10 K (○), where $f_c=0.003$. The solid lines through the points correspond to $t=1.99$ at 10 K and $t=1.33$ at 300 K.

$\zeta_R$ is the resistivity scaling exponent ($\zeta_R=0.975$ in two dimensions and 1.3 three dimensions); $r_h$ is the hopping length; $(r_h)^{\zeta_R}\sim(T_0/T)^{\zeta_R\gamma/\zeta}$, which contains the information about the fractal network (where $\gamma$ and $\zeta$ are the conductivity and the superlocalization exponent, described in more detail below).

The fit to Eq. (1) is shown in Fig. 2(b); at 10 K, we find $f_c=0.3\pm0.05\,\%$ and $t=1.99\pm0.04$, in agreement with the predicted universal value of $t\approx2$ for percolation in three dimensions.[1] At room temperature, however, $t=1.33\pm0.02$ (and $f_c=0.3$). The smaller value at room temperature arises from thermally induced hopping transport between disconnected (or weakly connected) parts of the network.

At 10 K and at room temperature, the values of the electrical conductivity of PANI-CSA/PMMA samples with $f\approx f_c$ are of the order of $10^{-5}$ S/cm and $10^{-3}$ S/cm, respectively; values which are quite high. For comparison, polyaniline blends made by dispersing intractable polyaniline in host polymers[12] show percolation only at much higher levels, $f_c\approx8.4\%$. In such samples, the room temperature conductivity at $f_c$ is five orders of magnitude lower, of the order of $10^{-8}$ S/cm.[12] More recent work has demonstrated that even with high quality soluble material, the morphology of the polyaniline can be controlled by proper choice of the solvent, neutral ad-

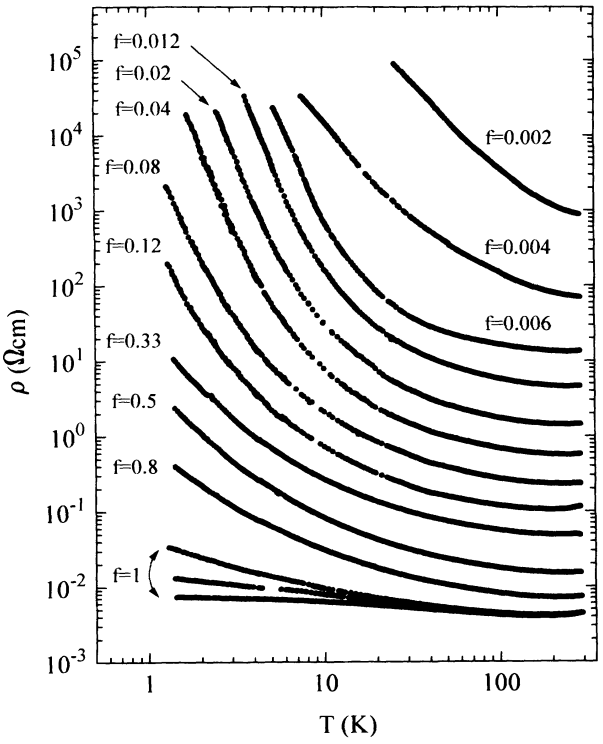


FIG. 3. $\mathrm{Log_{10}}$-$\mathrm{log_{10}}$ plot of resistivity ($\rho$) vs temperature of PANI-CSA/PMMA blends at various concentrations ($f$) of PANI-CSA ($0.002 < f < 1$).

ditives, and the dopant counterion. Although the results of these different choices have been characterized for pure polyaniline, studies of the corresponding effects in blends have only just begun.[20]

Although $f_c \approx 0.1$ vol % has been reported[21] for carbon-black-polymer blends the room temperature conductivity near $f_c$ is nearly four orders of magnitude less than that observed in PANI-CSA/PMMA blend. Similar values for both the percolation threshold (0.4 wt. %) and the critical exponent ($t \approx 1.3$, at room temperature) have been obtained from carbon-black-polyethylene-polystyrene blends, and attributed to the two dimensionality of the system.[22(a)] However, the conductivity obtained in filled polymer composites containing similar volume fractions of carbon-black[21,22(a)] or graphite particles[22(b)] near $f_c$ is of order $10^{-7}$ S/cm, again many orders of magnitude below that of PANI-CSA/PMMA at $f_c$.

### B. Temperature dependence of the resistivity of the network

The temperature dependence of the resistivity for PANI-CSA/PMMA blends is shown in Fig. 3 for $0.002 \leq f \leq 1$. The intrinsic nature of PANI-CSA as a metallic system near the boundary of the metal-insulator transition is characterized by the positive temperature coefficient of $\rho(T)$.[14] Although the positive temperature coefficient is restricted to somewhat higher temperatures upon dilution of PANI-CSA in PMMA,[11,14] it is remarkable that this metallic feature is observed even in samples containing volume fractions of PANI-CSA as low as

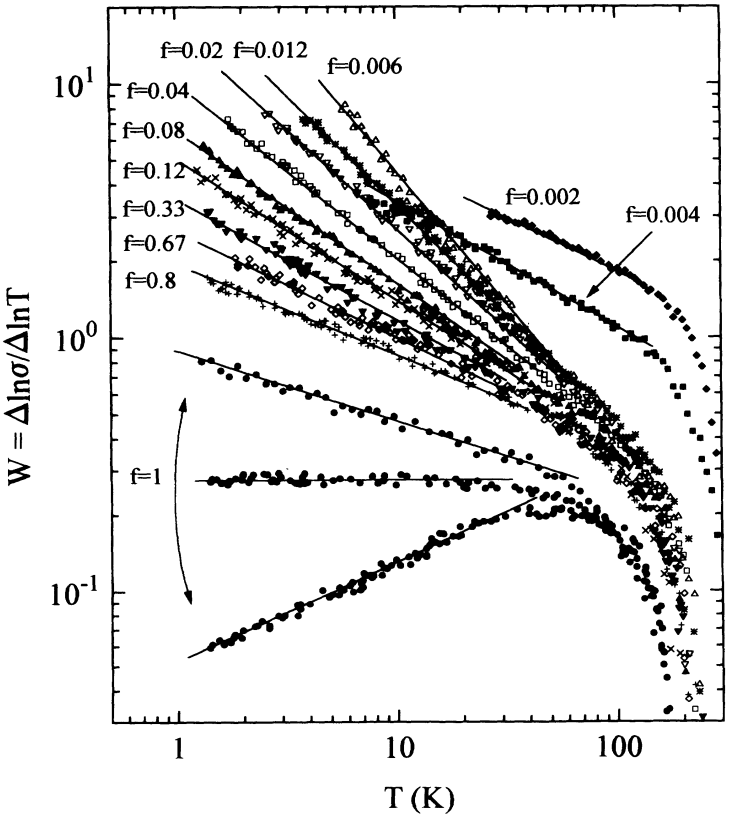


FIG. 4. $\mathrm{Log_{10}}$-$\mathrm{log_{10}}$ plot of $W = (\Delta \ln\sigma / \Delta \ln T)$ vs $T$ for $0.002 < f < 1$. The values of $T_0$ and $\gamma$ in Eq. (2) were determined from the straight lines using Eq. (4).

$f \approx 0.3\%$. This result indicates that even at such dilution, the PANI-CSA within the phase-separated network is comparable in quality to that of pure PANI-CSA.

According to variable range-hopping (VRH) theory,

$$\sigma(T) \propto \exp[-(T_0/T)^{\gamma}] , \tag{2}$$

where $T_0$ is the characteristic temperature that determines the thermally activated hopping among localized states at different energies. In conventional VRH which assumes exponentially localized states, $\gamma = 1/(d+1)$, where $d$ is the dimensionality of the system. For VRH on a percolating network, $\gamma$ is determined by the details of the complex connected network and the associated more rapid falloff of the wave functions.

The temperature dependence of the resistivity of PANI-CSA/PMMA blends can be classified into three separate concentration regimes.

(a) $0.01 \le f \le 1$; in this regime, $\gamma$ increases systematically from 0.25 to 1.

(b) $0.006 \le f \le 0.01$; in this regime, $\gamma = 1$.

(c) $0.002 \le f \le 0.006$; in this regime, $\gamma = \frac{1}{2}$.

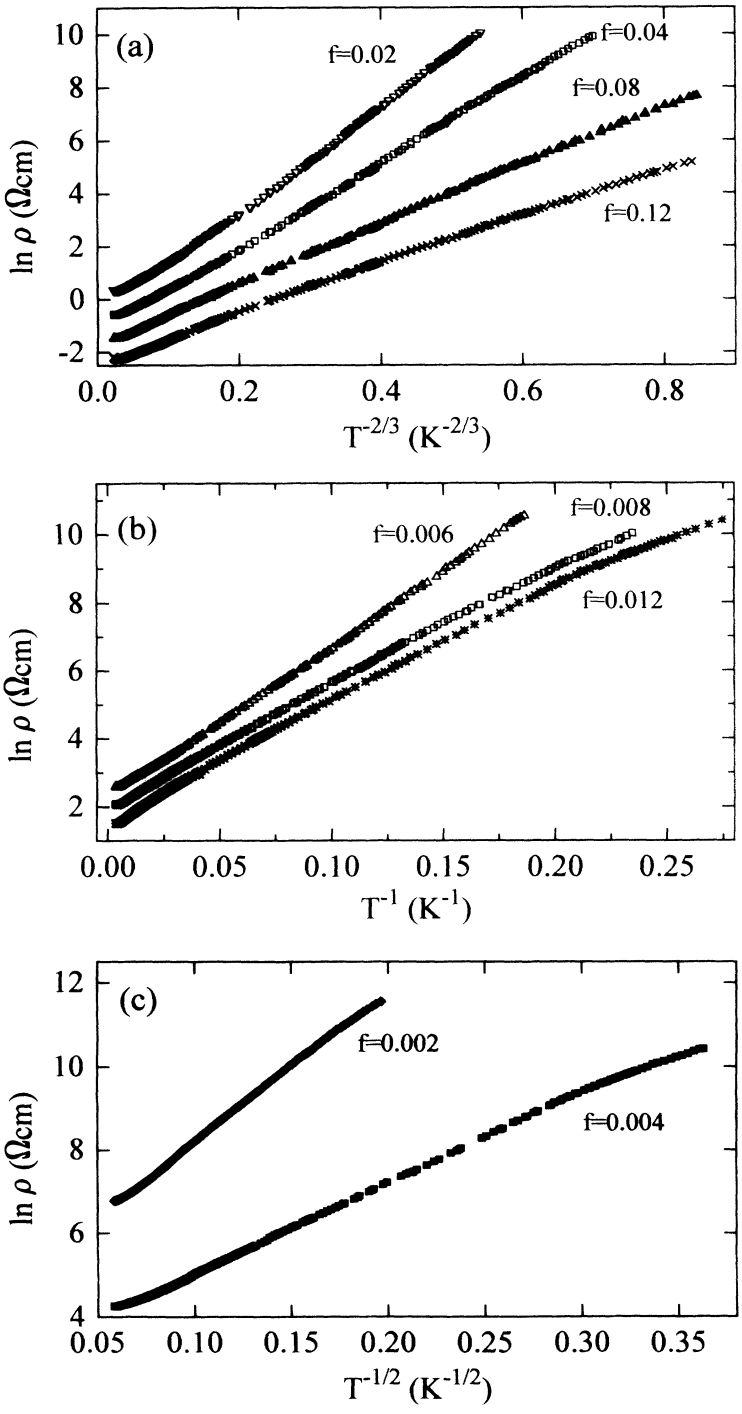


FIG. 5. Natural logarithm of $\rho(T)$ vs $T^{-\gamma}$, (a) $\gamma = \frac{2}{3}$ for $f = 0.12$, 0.08, 0.04, and 0.02; (b) $\gamma = 1$ for $f = 0.012$, 0.008, and 0.006; (c) $\gamma = \frac{1}{2}$ for $f = 0.004$ and 0.002.

### 1. *Temperature dependence of conductivity above the percolation threshold*

We define the logarithmic derivative of the conductivity

$$W(T)=T[d\ln\sigma(T)]/dT=\Delta\ln\sigma(T)/\Delta\ln T \quad (3)$$

and plot the data as $W(T)$ vs $T$. Figure 4 shows $W(T)$ vs $T$ for different volume fractions of PANI-CSA.[11,14] Using the $W(T)$ plot, one can obtain the parameters ($\gamma$ and $T_0$); from Eq. (2),

$$\log W(T)=A-\gamma\log T\ , \quad (4a)$$

$$A=\gamma\log T_0+\log\gamma\ . \quad (4b)$$

Pure PANI-CSA ($f=1$) is at the boundary of the disorder-induced metal-insulator ($M$-$I$) transition with $\rho(T)$ dependent upon the extent of disorder.[14] At the $M$-$I$ boundary, $W$ is constant indicating a power-law dependence for $\rho(T)$ while in the insulating regime close to the $M$-$I$ transition, $W$ follows Eq. 4(a) with $\gamma=\frac{1}{4}$. Upon dilution of PANI-CSA in PMMA, $\gamma$ increases systematically from $\gamma=0.25$ for $f\approx 1$ to $\gamma=1$ for $f=f_c$.

The approximate fits to the $\ln\rho\propto T^{-\gamma}$ dependence for selected volume fractions of PANI-CSA below 12% are shown in Figs. 5(a), 5(b), and 5(c). The results are consistent with the conclusions drawn from the $W$ versus $T$ plots and indicate that the exponent increases systematically upon lowering the volume fraction of PANI-CSA. The systematic variation of $T_0$ and $\gamma$ as a function of the volume fraction of PANI-CSA is shown in Fig. 6; $T_0$ is practically constant, and $\gamma$ increases systematically over the wide range of volume fractions above the percolation threshold. Both $T_0$ and $\gamma$ change dramatically when the network becomes disconnected at concentrations $f<f_c$.

The systematic increase of $\gamma$ from 0.25 to 1 upon dilution of PANI-CSA ($0.012\le f\le 1$) is not expected in the standard VRH model. However, since electrical transport in the blends takes place with in the convoluted and multiply connected PANI-CSA network, the role of the complex morphology must be taken into account.

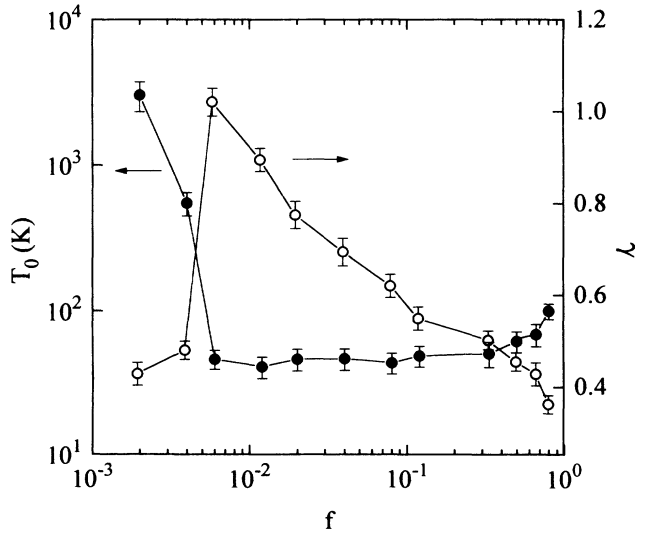


FIG. 6. $T_0$ and $\gamma$ vs the volume fraction ($f$) of PANI-CSA in PMMA.

Quite generally, percolating networks are known to be fractal for $f\approx f_c$. In our earlier studies of the morphology, we demonstrated that the PANI-CSA network in PMMA is needed fractal at concentrations close to $f_c$ and that the fractal dimensionality decreases as $f$ approaches $f_c$.[11] At higher concentrations, the network is a low-density *effective medium*; the network is complex and full of holes, but the mass distribution varies as $r^D$, where $D$ equals the spatial dimension.[11] These changes in microstructure with concentration must be included in an analysis of transport on such a network.

Levy and Souillard[15(a)] have shown that in a fractal structure, the wave functions are superlocalized, and decay as $\psi(r)\propto\exp[-(r/L_c)^{\zeta}]$, where $L_c$ is the localization length and $\zeta$ is the superlocalization exponent which is greater than unity (in Anderson localization $\zeta\approx 1$). Deutscher, Levy, and Souillard[15(b)] predicted that the temperature dependence of the electrical conductivity which results from VRH between superlocalized states would be of the form $\sigma(T)\propto\exp[-(T_0/T)^{\gamma}]$; where $\gamma=\zeta/(\zeta+D)\approx\frac{3}{7}$. Harris and Aharony[23] predicted that $\gamma$ is approximately 0.38 and 0.35 for two and three dimensions, respectively, for hopping transport in the superlocalized regime. The theory of VRH among superlocalized states was generalized by van der Putten *et al.*[21(b)] to include the Coulomb interaction; van der Putten *et al.* obtained $\gamma\approx 0.66$ and $\zeta\approx 1.94$ consistent with the experimental results in carbon-black-polymer composites.[21(b)] However, Aharony *et al.* argued that $\zeta=1.36$ in three dimensions[24] and suggested that the generalized VRH equation should be used in the superlocalized regime:

$$\sigma(T)=\sigma_0(T_0/T)^s\exp[-(T_0/T)^{\gamma}]\ . \quad (5)$$

However, due to the large uncertainty[24] in the value of "$s$" it is not possible to determine the values of $T_0$ and $\gamma$ unambiguously from Eq. (5).

Aharony *et al.* pointed out that *a priori* requisite for applying the fractal geometry near the percolation threshold is that the length scales satisfy the following condition: ($a\ll L_c\ll r_h\ll\xi_p$).[24] As described below, the localization length ($L_c$) can be obtained from the magnetic-field dependence of resistivity; at 4.2 K, $L_c\approx 25$ Å for the 0.4% PANI-CSA sample. The hopping length, $r_h(T)$, can be estimated from the following expression:[25]

$$r_h(T)=(\tfrac{1}{4})L_c(T_0/T)^{1/2}\ . \quad (6)$$

Substituting the appropriate values for $L_c$ and $T_0$ for the same 0.4% PANI-CSA sample, $r_h\approx 85$ Å at 4.2 K. The TEM micrograph for 0.5% PANI-CSA in PMMA indicates that the lower estimate for $\xi_p$ is approximately 400 Å. The value of the smallest unit ($a$) is the length of unit cell along the PANI chain direction, $a\approx 10$ Å. Hence, the conditions presented by Aharony *et al.* required for superlocalization of the electronic wave functions in a material with fractal network near the percolation threshold are satisfied:[24]

$$(a \ll L_c \ll r_h \ll \xi_0) \approx (10 < 25 < 85 < 400 \text{ Å}) . \quad (7)$$

In our previous studies,[11] where the percolation threshold was at 1.5% volume fraction PANI-CSA in PMMA, $\gamma = 0.66 \pm 0.4$ was observed for $0.0065 \leq f \leq 0.09$. This is consistent with the results presented here; again, we find $\gamma = 0.66 \pm 0.4$ for $0.02 \leq f \leq 0.1$. By decreasing $f_c$, the study of the systematic variation of $\gamma$ with concentration can be extended to much lower concentrations. These results, from a wider range of concentrations, indicate that the $\gamma = 0.66$ dependence is not unique to superlocalization near the percolation threshold. The experimental results shown in Fig. 6 show that the exponent of the temperature dependence of the conductivity in the superlocalized regime is sensitive to $D$ which in turn is determined by the morphology and the volume fraction of PANI-CSA in the system.

An alternative interpretation for this systematic increase in $\gamma$ is possible by introducing the concept of fractal character of the localized wave functions near the mobility edge.[26–28] In the standard VRH theory, the total number of states involved in the hopping conduction is assumed to be $x^d$ times the density of states per unit volume in a region of linear dimension "$x$" and the temperature dependence of conductivity is expressed by Eq. (2). Aoki[26] and Schreiber[28] have shown that near the mobility edge, the localized wave functions are fractal and that because of the fractal nature of the wave functions, the number of states involved in the hopping conduction behaves like $x^D$ where $D$ is the fractal dimensionality (rather than $x^d$). The conductivity resulting from variable range hopping among such spatially fractal localized wave functions is expressed by

$$\sigma(T) \propto \exp[-(T_0/T)^{1/(D+1)}] . \quad (8)$$

Since $D < d$, $\gamma$ is larger than usual values ($\frac{1}{4}$ for $3d$, etc.). Moreover, calculations by Schreiber and Grussbach has shown that $D$ decreases significantly with increasing disorder, yielding a further increase in the exponent of $(1/T)$ for increasing localization.[28(b)] The extent of disorder increases upon dilution of PANI-CSA by PMMA since the localization length decreases for concentrations which approach the percolation threshold.[11(b)] However, the presence of positive temperature coefficient of resistivity near room temperature, even for samples near the percolation threshold, indicates that the enhancement in disorder is not drastically affecting the intrinsic metallic properties of PANI-CSA upon dilution. Thus the change is $\gamma$ as a function of $f$ is probably dominated by the network (superlocalization) rather than by changes in the disorder in the PANI-CSA material within the network.

The $\sigma(T) \propto \exp[-(T_0/T)]$ dependence for samples near $f_c$ containing volume fractions of PANI-CSA between 0.6% and 1%, must result from other factors, since $\gamma = 1$ is outside the limits of superlocalization theory and $D$ is certainly greater than zero [see Eq. (8)].

Since the fibrillar links are the most resistive units in the network near the percolation threshold, charge transport through the links will dominate when the fibrillar diameter becomes comparable to the hopping length. As shown above, the hopping length is nearly 100 Å, which is comparable to the diameter of the fibrillar links observed in the TEM photographs. Thus, the $\sigma(T) \propto \exp[-(T_0/T)]$ dependence for volume fractions of PANI-CSA between 1% and 0.5% is probably due to transport in the fibrillar links. The $\sigma(T) \propto \exp[-(T_0/T)]$ dependence is typically observed when the dominant contribution to charge transport takes place by nearest-neighbor hopping (NNH).[25] It is not clear, however, why such a nearest-neighbor hopping transport should dominate within the fibrillar links.

#### 2. *Temperature dependence of conductivity below the percolation threshold*

The exponent, $\gamma(f)$, goes through a maximum at the percolation threshold; for samples containing volume fractions of PANI-CSA below 0.5%, the exponent decreases rapidly from 1 to $0.45 \pm 0.05$, as shown in Fig. 6. The $\ln\rho$ vs $T^{-1/2}$ fits for samples containing 0.4% and 0.2% of PANI-CSA are shown in Fig. 5(c).

This major change in $\gamma$ at the percolation threshold, where the connectivity of the PANI-CSA network breaks up, is consistent with the TEM results. When the volume fraction of PANI-CSA decreases below 0.5% the fibrillar diameter of the links between multiconnected regions decreases rapidly until the connected network cannot be sustained. At the point where the morphology changes to isolated blobs, the charge transport undergoes a transition to that typical of granular metallic systems.

The $\ln\rho \propto T^{-1/2}$ dependence observed for samples containing volume fractions of PANI-CSA from 0.4–0.1 % is typical of granular metals.[29] Although the factors leading to the $T^{-1/2}$ fit for granular metals are not completely understood, recent theoretical work by Cuevas *et al.* has shown that the low-temperature transport properties could be dominated by long-range Coulomb interaction rather than by charging effects (as previously believed).[30] However, more theoretical work is necessary to understand the possible implications of superlocalization on the conductivity in this unusual regime in which the blobs appear to be locally self-similar but disconnected from one another.

### C. Magnetoresistance in the network near the percolation threshold

Recent theoretical work has shown that experimental studies of high-field magnetotransport in a percolating medium can provide insight into the relationship between microstructure and charge transport.[19] The magnetoresistance (MR), at 4.2 K, for samples containing volume fractions of PANI-CSA from 1.5% to 0.4% is shown in Fig. 7. The $H^2$ dependence of the positive MR at low fields, typical of that observed in VRH transport, is due to the shrinkage in the overlap of the wavefunctions of the localized states in the presence of the magnetic field.[25] The temperature dependences of the MR for samples containing 12% and 4% of the PANI-CSA, as typical examples of the large difference in the MR

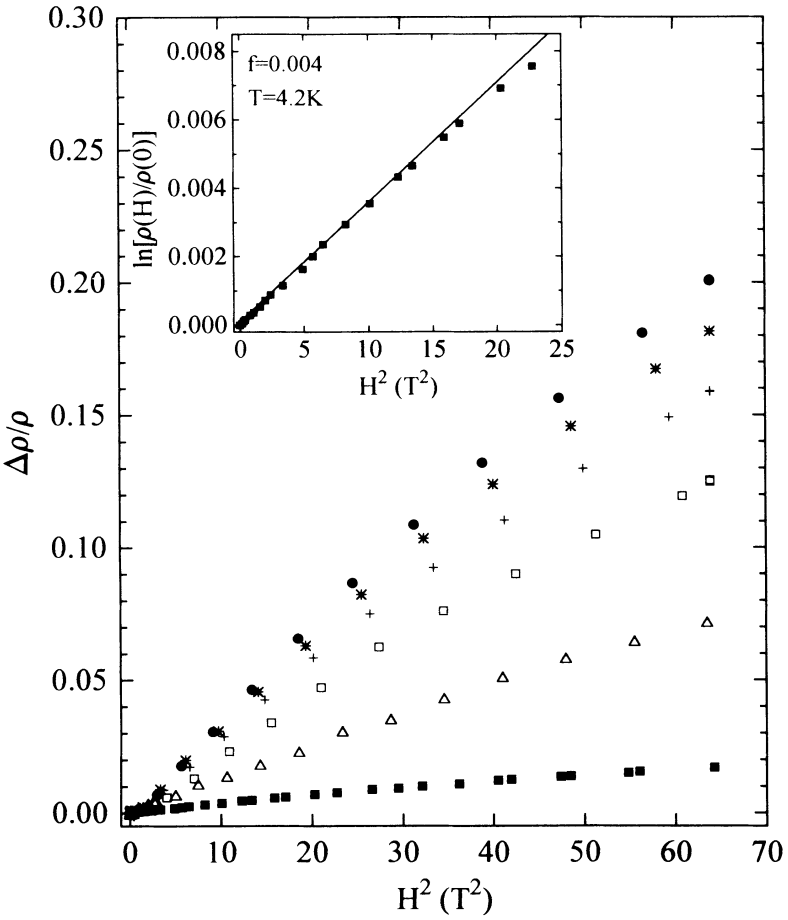


FIG. 7. Magnetoresistance $[\Delta\rho/\rho(0) = \{\rho(H)-\rho(0)\}/\rho(0)]$ vs $H^2$ for $f=0.015$(●), 0.012(✱),0.01(+),0.008(□),0.006(△), and 0.004(■), all at 4.2 K. The inset shows the natural logarithm of $\{\rho(H)/\rho(0)\}$ vs $H^2$ for $f=0.004$ at $T=4.2$ K. The solid line is the linear fit to Eq. (9).

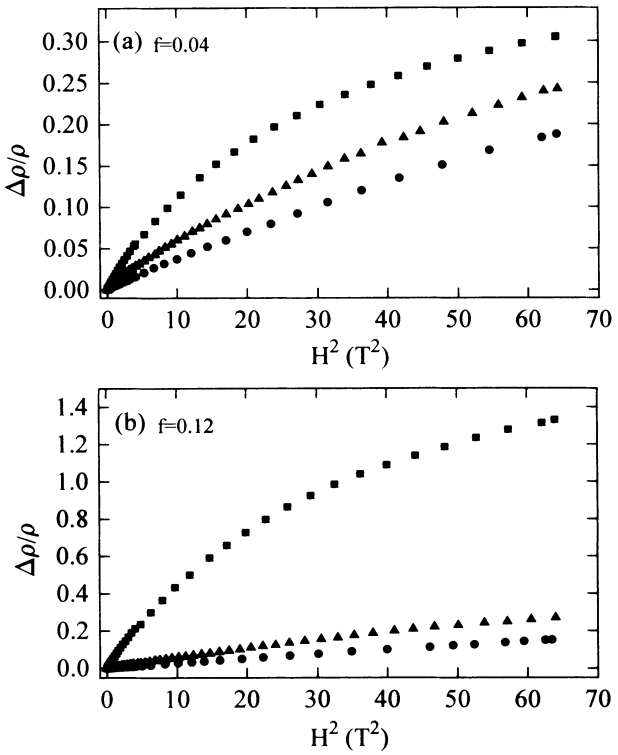


FIG. 8. Magnetoresistance $[\Delta\rho/\rho(0)=\{\rho(H)-\rho(0)\}/\rho(0)]$ vs $H^2$ at 4.2 K (●), 2.5 K (▲), and 1.4 K (■) for (a) $f=0.04$ and (b) $f=0.12$.

behavior at higher and lower volume fractions of PANI-CSA, are shown in Figs. 8(a) and 8(b). Finally, the variations of MR, at 4.2 and 1.4 K, as a function of the volume fraction of PANI-CSA from 100 to 0.4% are shown in Fig. 9.

The inset of Fig. 7 shows the field dependence of the resistivity for a 0.4% PANI-CSA sample at 4.2 K. In

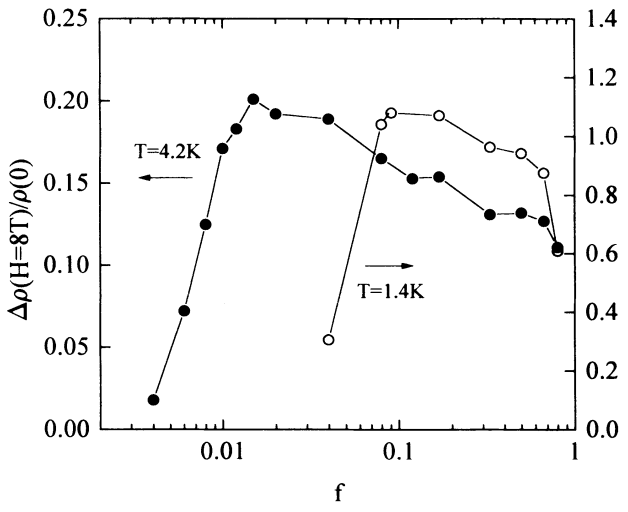


FIG. 9. Magnetoresistance $[\Delta\rho(H=8T)/\rho(0)=\{\rho(H=8T)-\rho(0)\}/\rho(0)]$ plotted as function of the volume fraction ($f$) of PANI-CSA in PMMA at 4.2 and 1.4 K for $1<f<0.004$.

VRH theory, the temperature and magnetic-field dependences of this quantity can be expressed as follows:[25]

$$\ln[\rho(H)/\rho_0]=t(e/\hbar c)^2 L_c^4 (T_0/T)^{3\gamma} H^2 , \quad (9)$$

where $t=0.0015$ for $\gamma=1/2$, $\hbar$ is Planck constant, $e$ is the electronic charge, $c$ is the velocity of light. The localization length for the 0.4% PANI-CSA sample can be calculated from the slope of the straight line in the inset of Fig. 7 (using $T_0 \sim 800$ K as obtained from the temperature dependence of the resistivity). Thus, near the percolation threshold, $L_c \approx 25$ Å at 4.2 K.

We note that the magnitude of the positive MR shows a temperature-dependent maximum upon decreasing the volume fraction of PANI-CSA. Above 4.2 K the MR is rather low for both 100% PANI-CSA and for the blends. At 4.2 K, the MR is maximum at 1.5% PANI-CSA; at 1.4 K, the MR is maximum at 8% PANI-CSA.

Recent theoretical work has proposed a discrete model for magnetotransport in percolating systems.[19] This model, which assumes that the conducting component has a closed Fermi surface and that the MR saturates at high fields, predicts a large MR in the vicinity of the percolation threshold. This is contrary to the predictions of effective-medium theory in which there is no MR near the percolation threshold.[31,32] For insulating PANI-CSA (100%), the MR tends to saturate at 8 T,[14(b)] but it is not known whether the Fermi surface of PANI-CSA is open or closed. In order to address this question, we have carried out the MR measurements in many PANI-CSA/PMMA samples ($f \approx 0.4-1.5$ vol %) near the percolation threshold in which the volume fraction of PANI-CSA varies by 0.1% from sample to sample. At 4.2 K, the MR increases systematically upon dilution from 100% to 1.5% of PANI-CSA, while below 1.5% the MR decreases rapidly as $f$ approaches the percolation threshold. However, at 1.4 K the MR is much larger than at 4.2 K and the maximum in MR shifts to nearly 8% PANI-CSA sample.

The increase in MR upon dilution is consistent with the VRH model since the overlap of wave functions of localized states decreases due to superlocalization of the fractal network upon decreasing the volume fraction of PANI-CSA.[25,15] As noted earlier, when the volume fraction of PANI-CSA decreases below 1.5% the diameter of links decreases and the interblob distance increases; consequently the hopping length and the diameter of links becomes rather similar. At temperatures below 4.2 K the hopping length further increases, and the maximum in MR shifts to higher volume fractions of PANI-CSA (larger diameter of the fibrillar links), consistent with the observation at 1.4 K. This is also consistent with the $\ln\sigma \propto 1/T$ dependence for samples containing volume fractions of PANI-CSA from 1% to 0.5%. The rapid decrease in MR on approaching the percolation threshold is in qualitative agreement with effective medium theory; the data do not support the discrete model.

## IV. CONCLUSIONS

Transmission electron microscopy studies and conductivity measurements of PANI-CSA/PMMA blends indicate that the volume fraction of PANI-CSA at the percolation threshold is approximately 0.3%. The conductivity near percolation threshold is $3\times10^{-3}$ S/cm at room temperature. The formation of a self-assembled interpenetrating network of PANI-CSA results in a low percolation threshold with rather high conductivity at threshold in comparison with other percolating systems. The typical positive temperature coefficient of the resistivity of PANI-CSA remains even at volume fractions near the percolation threshold.

The value of $\gamma$ in the temperature dependence of the conductivity, $\ln\sigma \propto T^{-\gamma}$, increases systematically from 0.25 to 1 upon dilution, indicating that transport of the network depends on the morphology and connectivity of the network. Near $f_c$, the length scales $[(a \ll L_c \ll r_h \ll \xi_p) \approx (10 < 25 < 85 < 400$ Å$)]$ satisfy the criteria for applying the superlocalization theory of transport on a fractal geometry. Near $f_c$, we find $\gamma=1$. In this regime, where the hopping length and the diameter of fibrillar links are similar, the $\ln\rho \propto 1/T$ dependence is typical of nearest-neighbor hopping. When the concentration is decreased below the percolation threshold where the fibrillar network breaks up, $\gamma=\frac{1}{2}$. In this disconnected regime below $f_c$, the $T^{-1/2}$ dependence of the conductivity is typical of that of granular metals.

The positive MR increases upon decreasing the volume fraction of PANI-CSA; when the fibrillar diameter and the hopping length become comparable, the MR decreases rapidly. The maximum in MR at 4.2 and 1.4 K are at 1.5% and 8% PANI-CSA, respectively. The negligible MR near threshold is in qualitative agreement with effective-medium theory but contrary to the large MR predicted according to the recent discrete model near the percolation threshold.

## ACKNOWLEDGMENTS

This work was partially supported by the MRL program of the National Science Foundation through Grant No. NSF-DMR 91-23048, and partially supported by a research grant from the Electric Power Research Institute (EPRI). The PANI-CSA/PMMA blends were supplied by UNIAX Corporation.

[1] A. Aharony and D. Stauffer, *Introduction to Percolation Theory*, 2nd ed. (Taylor & Francis, London, 1993), and references therein.

[2] B. Bridge and T. Tee, Int. J. Electron. **6**, 785 (1990), and references therein.

[3] S. De Bondt, L. Froyen, and A. Deruyttere, J. Mater. Sci. **27**, 1983 (1992).

[4] F. Carmona, Physica A **157**, 461 (1989), and references therein.

[5]S. H. Munson-McGee, Phys. Rev. B **43**, 3331 (1991).
[6]A. Fizazi, J. Moulton, K. Pakbaz, S. D. D. Rughooputh, Paul Smith, and A. J. Heeger, Phys. Rev. Lett. **64**, 2180 (1990); Yasuo Y. Suzuki, A. J. Heeger, and P. Pincus, Macromolecules **23**, 4730 (1990).
[7]A. Andreatta, A. J. Heeger, and Paul Smith, Polym. Commun. **31**, 275 (1990).
[8]Y. Wang and M. F. Rubner, Macromolecules **25**, 3284 (1992).
[9]M. Makhlouki, M. Morsli, A. Bonnet, A. Conan, A. Pron, and S. Lefrant, J. Appl. Polym. Sci. **44**, 443 (1992).
[10](a) Y. Cao, P. Smith, and A. J. Heeger, Synth. Met. **48**, 91 (1992); (b) C. Y. Yang, Y. Cao, Paul Smith, and A. J. Heeger, *ibid.* **53**, 293 (1993); (c) Y. Cao *et al.* (unpublished).
[11](a) Reghu M., C. O. Yoon, C. Y. Yang, D. Moses, A. J. Heeger, and Y. Cao, Macromolecules **26**, 7245 (1993); (b) C. O. Yoon, Reghu M., D. Moses, A. J. Heeger, and Y. Cao, Synth. Met. **63**, 47 (1994); (c) Phys. Rev. B **48**, 14 080 (1993).
[12](a) C. K. Subramaniam, A. B. Kaiser, P. W. Gilberd, and B. Weβling, J. Polym. Sci. B **31**, 1425 (1993); (b) R. Pelster, G. Nimtz, and B. Weβling, Phys. Rev. B **49**, 12 718 (1994).
[13]K. Levon, A. Margolina, and A. Z. Patashinsky, Macromolecules **26**, 4061 (1993).
[14](a) Reghu M., Y. Cao, D. Moses, and A. J. Heeger, Phys. Rev. B **47**, 1758 (1993); (b) Reghu M., C. O. Yoon, Y. Cao, D. Moses, and A. J. Heeger, *ibid.* **48**, 17 685 (1993).
[15](a) Y. E. Levy and B. Souillard, Europhys. Lett. **4**, 233 (1987); (b) G. Deutscher, Y. E. Levy, and B. Souillard, *ibid.* **4**, 577 (1987).
[16](a) A. Aharony and A. B. Harris, Physica A **163**, 38 (1990); (b) **205**, 335 (1994), and references in (1).
[17]A. Aharony and A. B. Harris, Physica A **191**, 365 (1992).
[18]H. Grussbach and M. Schreiber, Physica A **191**, 394 (1992).
[19]A. K. Sarychev, D. J. Bergman, and Y. M. Strelniker, Phys. Rev. B **48**, 3145 (1993); D. J. Bergman and A. K. Sarychev, Physica A **200**, 231 (1993).
[20](a) Y. Cao, in Proceedings of the International Conference on the Science and Technology of Synthetic Metals (ICSM '94), Seoul, Korea [Synth. Met. (to be published)]; (b) A. G. MacDiarmid, *ibid.*
[21](a) M. A. Michels, J. C. M. Brokken-Zijp, W. M. Groenewoud, and A. Knoester, Physica A **157**, 529 (1989); (b) van der Putten, J. T. Moonen, H. B. Brom, J. C. M. Brokken-Zijp, and M. A. J. Michels, Phys. Rev. Lett. **69**, 494 (1992); **70**, 4161 (1993); (c) H. B. Brom, European patent No. EP 0 370 586 A2; (private communication).
[22](a) F. Gubbels, R. Jerome, Ph. Teyssie, E. Vanlathem, R. Deltour, A. Calderone, V. Parente, and J. L. Bredas, Macromolecules **27**, 1972 (1994); (b) A. Quivy, R. Deltour, A. G. M. Jansen, and P. Wyder, Phys. Rev. B **39**, 1026 (1989); M. Mehbod, P. Wyder, R. Deltour, C. Pierre, and G. Geuskens, *ibid.* **36**, 7627 (1987).
[23]A. B. Harris and A. Aharony, Europhys. Lett. **4**, 1355 (1987).
[24]A. Aharony, O. Entin-Wohlman, and A. B. Harris, Physica A **200**, 171 (1993); Phys. Rev. Lett. **70**, 4160 (1993).
[25]B. I. Shklovskii and A. L. Efros, *Electronic Properties of Doped Semiconductors* (Springer, Heidelberg, 1984); T. G. Castner, in *Hopping Transport in Solids*, edited by M. Pollak and B. I. Shklovskii (North-Holland, Amsterdam, 1991).
[26]H. Aoki, J. Phys. C **16**, L205 (1983); Phys. Rev. B **33**, 7310 (1986).
[27]C. M. Soukoulis and E. N. Economou, Phys. Rev. Lett. **52**, 565 (1984).
[28](a) Michel Schreiber, Phys. Rev. B **31**, 6146 (1985); (b) M. Schreiber and H. Grussbach, Philos. Mag. B **65**, 707 (1992).
[29]M. Pollak and C. J. Adkins, Philos. Mag. B **65**, 855 (1992).
[30]E. Cuevas, M. Ortuno, and J. Ruiz, Phys. Rev. Lett. **71**, 1871 (1993).
[31]B. Ya. Balagurov, Fiz. Tverd. Tela **28**, 3012 (1986) [Sov. Phys. Solid State **28**, 1694 (1986)].
[32]D. Stroud and F. P. Pan, Phys. Rev. B **13**, 1434 (1976).

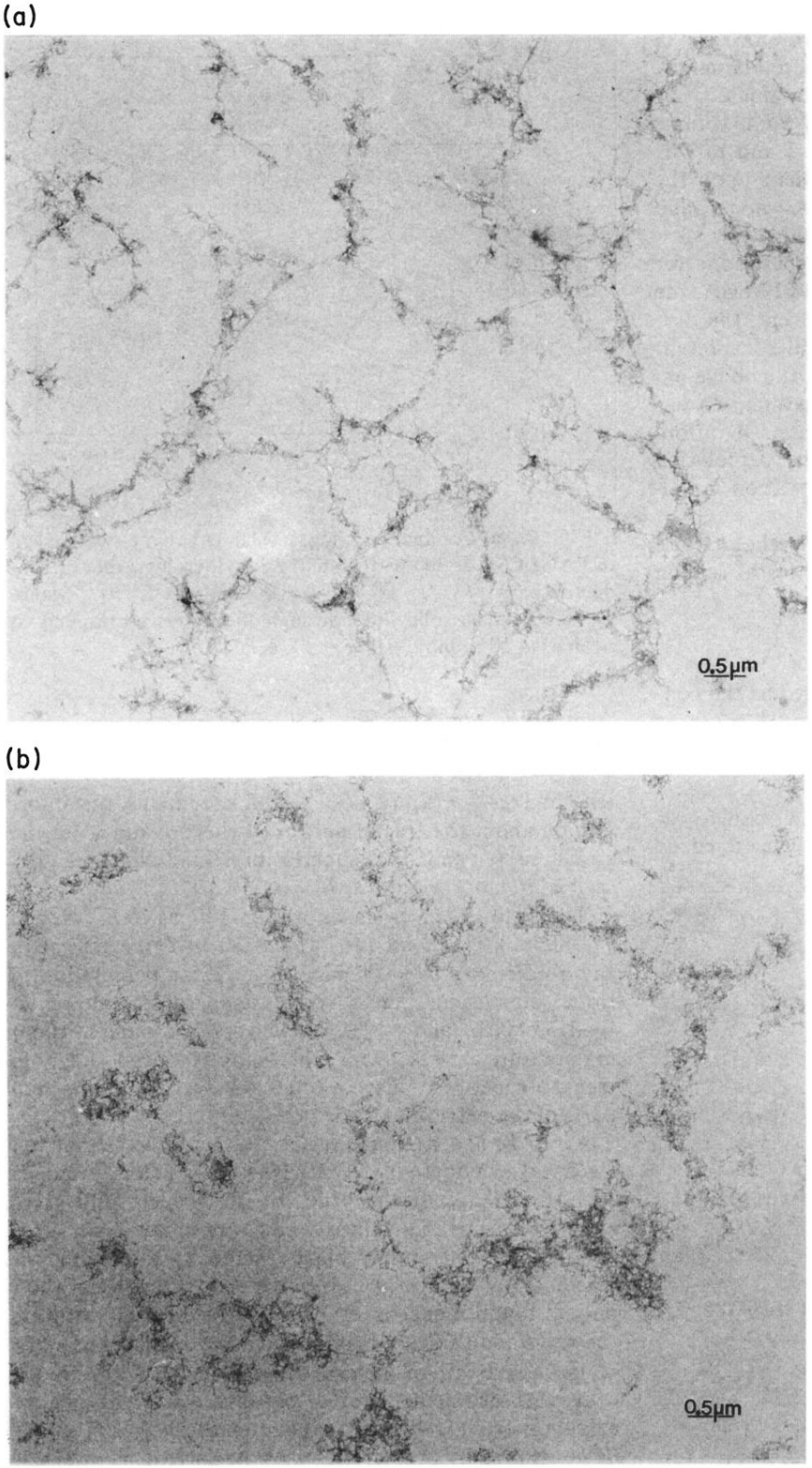


FIG. 1. Transmission-electron micrographs of extracted PANI-CSA/PMMA polyblend films containing (a) $f=0.005$ and (b) $f=0.0025$ PANI-CSA.